Calculation of Radio Interference for Unconventional High Surge Impedance Loading Transmission Lines

Mushfiqul Abedin Khan, Mona Ghassemi, and Saikat Chowdhury
Department of Electrical and Computer Engineering
The University of Texas at Dallas
Richardson, TX, USA

Abstract —It is crucial to study the effects of corona discharge during the design of an overhead transmission line. These effects include power losses, radio interference (RI), television interference (TVI), and audible noise (AN). Extra high voltage conventional transmission lines above 300 kV are designed to have more than one conductor per phase to form conductor bundles which causes the electric field stress on the subconductors to be reduced, which in turn reduces the corona effects. Conventional high surge impedance loading (HSIL) lines consist of a higher number of subconductors with a larger bundle radius which effectively increases its transmission capacity. On the other hand, unconventional HSIL lines have demonstrated the potential to deliver higher natural power which surpasses that of both conventional and conventional HSIL lines. The term unconventional refers to the asymmetrical arrangement of the subconductors in bundles. With the increased number of subconductors per bundle, HSIL lines may have higher electric field stress on the conductors' surface leading to greater corona effects. In this paper, the RI from unconventional lines are evaluated and analyzed.

Keywords— Radio Interference (RI), high surge impedance loading (HSIL), unconventional HSIL lines, corona discharge, natural power.

I. INTRODUCTION

Corona discharges result from the partial breakdown of air around high-voltage conductors. This causes power losses, electromagnetic interferences such as radio (RI) and television interference (TVI), and audible noise (AN). In overhead transmission lines, corona can be distinguished as glow corona and streamer corona, of which, the latter produces RI between 0.5 to 1.6 MHz. As a result, radio station receivers around transmission lines detect this interference as noise. To overcome this, the RI level has to be lower than a certain threshold value at the receiver location. This threshold is determined by the signal-to-noise ratio (SNR). In the USA, for signals with strength greater than 54 dB, for reasonable reception, the minimum recommended SNR is 24 dB. In Canada, this value is 22 dB for fair weather conditions in the suburbs. This value can be decreased by 3 dB for rural areas and increased by 10 dB for urban regions [1].

Deregulation and inadequate foresight in power sector expansion planning have led to significant changes in the load flow patterns of transmission lines. Additionally, the integration of renewable resources in specific regions in the grid has resulted in the overload of certain lines, while others remain underutilized. Furthermore, investors prioritizing the generation

and distribution sectors for immediate returns result in deferred contributions to the transmission sector, bringing the U.S. power system dangerously close to its maximum loadability and stability margins [2-4]. It has been shown in a recent study that for America to reach net-zero emissions by 2050, the transmission capacity must be increased by 60% within 2030 and tripled by 2050, to include further solar and wind energy resources into the grid [5]. In light of the mentioned constraints and objectives, it is crucial to enhance the power delivery capacities of the transmission lines. A viable option can be found in high voltage direct current (HVDC) lines, because of their potential to reach high power capacity. However, the unavailability of HVDC circuit breakers (CBs) which are commercially produced has rendered this choice unfeasible. Thus, the focus shifts to extra high voltage AC (EHV AC) lines in terms of increasing transmission capacity. Generally, the use of series and shunt capacitor banks reduces the line reactance and injecting reactive power has seen the enhancement of line loadability in such cases. This would, however, be a costly solution [2]. High surge impedance loading (HSIL) lines are considered to be a viable alternative to increase natural power without the incorporation of reactive compensation techniques [2]. Conventional HSIL lines have a greater bundle radius and a higher number of subconductors per bundle than conventional lines. The unconventional HSIL lines have a nonuniform disposition of the subconductors in the bundled phases compared to the symmetrical arrangement in a conventional or conventional HSIL line. The unconventional lines have shown the potential to improve line loadability. Before implementing these new unconventional HSIL lines, many constraints must first be addressed during the design stage, including the corona discharge effects including RI. Thus, accurate estimation of these values is crucial. These effects become more pronounced compared to acceptable levels if the conductor surface electric field exceeds a particular boundary value derived from the corona onset gradient, highlighting the importance of accurately calculating the electric field on the surface of the conductors. This is performed using a novel method we have introduced in one of our papers [6]. A further limitation is that the empirical formula and methods currently available for calculating RI due to corona have been exclusively derived for traditional bundled configurations. These models may not be reliable for the unconventional HSIL lines under discussion [2].

In this paper, the target is to develop accurate models for evaluating the effects of RI in unconventional HSIL lines.

This work was supported in part by the National Science Foundation (NSF) under Award #2306098.

II. METHOD

A. Corona Discharge

Corona discharge in transmission lines is the partial discharge of air due to high voltages in and around conductors. It occurs when the subconductor surface electric field exceeds a threshold based on the corona onset gradient. Under atmospheric pressure, this threshold for dry air is 30 kV/cm. For transmission line designs, however, the corona onset gradient is considered to be 20 kV/cm [7]. It is therefore desirable to maintain low conductor surface electric field stress levels to prevent corona discharge effects even under adverse weather conditions. However, there are cost limitations that make it difficult to minimize them.

B. Electric Field Levels

To determine if the conductor surface electric field is greater than the threshold corona onset gradient level, it is critical to precisely calculate it. The classical method of finding the electric field on the surface of the conductors is to calculate Maxwell's Potential Coefficients first and then use these values to evaluate the surface potential values. Each of the conductors is modeled using single line charges having a charge of q, surface potential V, and connected using q = CV, where C is the capacitance of the line. This equation is often rearranged as [P][q] = [V] for n subconductors per bundle, where [P] represents Maxwell's potential coefficients. The asymmetrical arrangement of the unusual HSIL transmission lines and the impact of the additional subconductors and phases are not taken into account by this method. In a novel approach, as we have discussed in another paper [6], the n subconductors are each modeled using n_m line charges placed symmetrically around a hypothetical cylinder having radius r/2, centered on the conductor center, thereon setting the potential at n_m points on the conductor surface, where r stands for the radius of the subconductor. Then, the conductor surface potential for each point P can be calculated. Fig. 1 shows the arrangement of the line charges and the assumed cylinder used to model the conductor's electric field.

$$E(P) = \sum_{i=1}^{n \times n_m} \frac{q_i}{2\pi\varepsilon_0 \left| \overrightarrow{r_p} - \overrightarrow{r_i} \right|^2} \left(\overrightarrow{r_p} - \overrightarrow{r_i} \right) \tag{1}$$
 where, q_i is the charge on the i^{th} line charge, and $\overrightarrow{r_p}$ and $\overrightarrow{r_i}$ are

where, q_i is the charge on the i^{th} line charge, and $\overrightarrow{r_p}$ and $\overrightarrow{r_t}$ are the distances to the line charges and the potential points from the center of the subconductor.

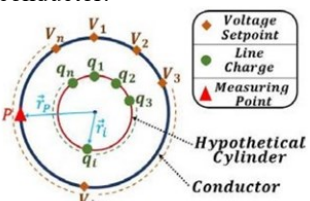


Fig. 1. Model of the subconductors using n_m line charges to determine the conductor surface electric field.

C. Radio Interference

Usually, for transmission lines at a voltage level greater than 230~275 kV, corona discharge occurs resulting in corona power loss, audible noise (AN), and electromagnetic interference (EMI). EMI can be classified into two main categories, namely RI and TVI. The former occurs due to streamer or pulse-type corona creating interference in the range

of 0.5~1.6 MHz which introduces noise in radio signal receivers. Free electrons and positive ions are created under high electric field stress. Initially, a few electrons exist which increase in number due to an avalanche of free electrons that start moving towards the anode. This causes a large and sudden increase in current which quickly reduces to a low value as the electric field becomes less intense. The formation of large and heavy stationary space charge clouds causes a reduction in the net electron velocity which results in a pulsating current in the electric field. The pulses formed to reach the peak value in a short time and fall off at a relatively slower rate. In the positive and negative half cycles of AC excitation, such pulses are formed based on which the response of the radio receivers is estimated besides modeling the radio interference. As the pulses diminish, factors such as wind cause the stationary ions to drift to one side, or as recombination with free electrons neutralizes the cations, the electric field reaches large values again, resulting in a repetition of the pulses. This repetition rate can be enhanced by moist conditions, which is why the corona effects become more dominant under rainfall [1]. The challenge involved with radio interference lies in placing the receivers adequately far from the transmission line laterally - thus ensuring that the noise produced by the line is sufficiently low at the receiver location, thereby achieving a standard quality of reception. The lateral RI profile should therefore be used to carefully evaluate the right-of-way (ROW) while designing a line as shown in Fig. 2.

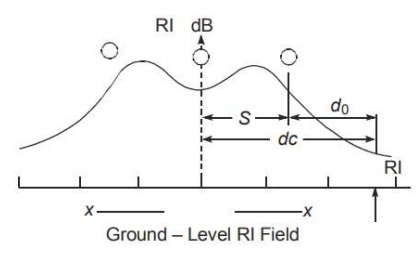


Fig. 2. Lateral RI profile for a 3-phase transmission line

The RI limits are set by the signal-to-noise ratio (SNR) at the receiver ends. In the USA, broadcast transmissions with a minimum strength of 54 dB are required to maintain a minimum SNR of 24 dB at the receiving end. The RI level can be calculated by the empirical formulae determined by various organizations based on their collected data. The empirical formula by CIGRE relates RI with conductor radius, maximum conductor surface electric field, frequency, weather, and the gap between the conductor and the receiver. For conductor i, RI is

$$RI_i(dB) = 3.5g_m + 6d - 33\log_{10}\frac{D_i}{20} - 30$$
 (2)

where g_m is the maximum voltage gradient on the surface of the conductor in kV/cm, D_i is the distance between the conductor and receiver in m, and d is the conductor diameter in cm. This provides a reliable estimate at a frequency of 0.5 MHz, D_i greater than 20 m, subconductor count per bundle less than or equal to 4, ratio of the bundle spacing to the subconductor diameter between 12~20, and for moderate weather conditions. The number of subconductors per bundle for the unconventional line under discussion is 8, thereby effectively eliminating the use of this method for calculating RI. Another empirical formula to be considered is the one by the Bonneville Power

Administration (BPA) [8]. Considering our novel method of evaluating the conductor surface electric field, the empirical formula by BPA can be applied to our proposed unconventional HSIL line to determine the RI profile which is given by:

$$RI = 46 + 120 \log_{10} \left(\frac{E_{max}}{17.56} \right) + 40 \log_{10} \left(\frac{2r}{3.51} \right) dB (1\mu V/m)$$
 (3)

where, E_{max} is the maximum conductor surface electric field, and r is the subconductor radius. For a CISPR standard quasipeak receiver at 1 MHz consisting of a horizontal loop antenna at a height of 1 m above the ground and a distance of 15 m from the considered phase under good weather, (3) can be used to calculate RI noise levels. Correction factors can then be added to the value found depending on parameters such as distance from the phase D, altitude levels A, and measurement frequency f. For measurable rain, 25 dB can be added to the value found in (3) to correct for the weather conditions. For altitude levels greater than 0 km above sea level, A/300 dB is added. The correction factor for different measurement frequencies other than 1 MHz is $10[1 - (log 10f)^2] dB$. The RI level changes with distance based on a correction factor of $C_2 - C_1 dB$, where C_2 is a constant for the line under consideration, and C_1 is a constant for a line with reference parameters. These are given by

$$C_i = 10 \log_{10}(DW^2 + ESU^2 + EIND^2) dB$$
, $i = 1,2$ (4) where DW is the direct wave, ESU is the surface wave, and

EIND is the induction field component, found using:

$$DW = \begin{cases} \frac{H}{k_0 D}, & for \ D \le \frac{12Hh_a}{\lambda} \\ \frac{H}{k_0 D} \frac{12Hh_a}{\lambda D}, & for \ D > \frac{12Hh_a}{\lambda} \end{cases}$$
 (5)

where H and h_a are the conductor and antenna heights, and Dis the distance from the antenna to the conductors in meters. λ

is the wavelength in meters, and
$$k_0=2\pi/\lambda$$
. ESU and EIND is
$$ESU=\frac{g(\Delta)H}{k_0D} \eqno(6)$$

 $g(\Delta) = (2 + 0.3\Delta)/(2 + \Delta + 0.6\Delta^2)$ $\Delta =$

$$52.5D/\sigma_g \lambda^2$$
. Here, σ_g is the ground conductivity in mS/m.
$$EIND = \frac{H}{(k_0 D)^2}$$
 (7)

 C_1 can be found using D = 21.04 m, f = 1 MHz, $\sigma_g = 4$ mS/ m and $h_a = 1$ m. For each of the phases, the RI noise levels are calculated using (3) to (7). The resultant RI profile is then determined by considering the maximum RI value among each of the phases for the specific points.

III. CASE STUDIES

In our study, we have considered an existing 3-phase, 500 kV conventional overhead transmission line, as well as our recently proposed revolutionary design of a 3-phase unconventional HSIL line at the same voltage level [9].

A. 500-kV Conventional Three Phase Transmission Line

Fig. 3 shows the 500 kV, 3-phase conventional transmission line which is the base case for our study [10]. The phases each consist of 4 subconductors separated by a 45 cm bundle spacing and the distance between the phases is 12.3 m. The subconductors used have a diameter of 26.82 mm. The height of each phase is 28 m from the surface of the ground.

B. A 500 kV Three Phase Unconventional Transmission Line

Fig. 4 shows our recently proposed 3-phase, 500 kV, unconventional HSIL line which consists of 8 subconductors per phase. The diameter of the subconductors is 20.93 mm and the phase-gap is about 8.12 m. For the outer phases, their average height is about 31.37 m, and that of the middle phase is about 24.29 m. The phases are arranged in an inverted delta configuration (IDC). Unconventional refers asymmetrically arranged nature of the sub-conductors compared to the symmetrical arrangement of a conventional line. This new design has shown the potential to deliver a higher natural power compared to the conventional line. For both lines, σ_a is taken as 10 mS/m.

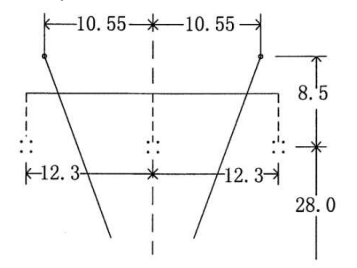


Fig. 3. Conductor configuration for the 500 kV conventional line

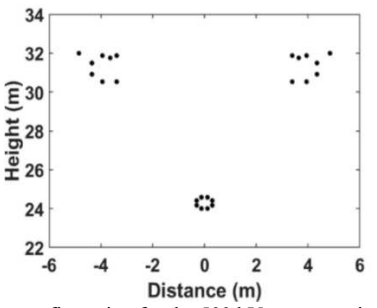


Fig. 4. Conductor configuration for the 500 kV unconventional HSIL line.

IV. SIMULATION RESULTS

We first considered the Corona and Field Effects software (CAFE31) by BPA to estimate the RI profile for the conventional line. This result was then used to validate the code we developed employing the model of Fig.1. The RI profile for the newly proposed unconventional line was then found using our novel method for measurement frequencies of 500 kHz, 5 MHz, and 20 MHz, respectively. Figs. 5 and 6 show the results for the conventional line from the CAFE31 software and our code, respectively. Fig. 7 shows the RI profile we have evaluated for our unconventional HSIL line based on our novel approach. It can be seen from the above results that for each considered measurement frequency, the RI of the unconventional line exceeds that of the conventional line by about 7~12 dB. It is also understood that for a 54 dB signal in the U.S., the noise level can be at most 30 dB for adequate signal reception. This for the conventional line is at distances of about 235 m and 25 m from the outer phase, for measurement frequencies of 0.5 and 5 MHz, respectively. For the unconventional line, the associate distance values are 690 m and 125 m. For 20 MHz, the noise level is below 30 dB for all distances. It is worth noting that in one of our papers [11], we discussed RI for unconventional lines, but the results presented in this paper are much closer to the ones from the CAFE31 software, which validated our work for the conventional line. Besides RI, other electrical, mechanical, and structural line design aspects of this new line and its implementation in transmission expansion planning should be carefully studied. We did some [12-20] and are studying others; live line working [21, 22] for the new line can be challenging.

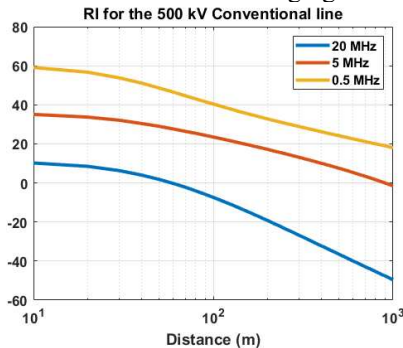


Fig. 5. RI profile for the conventional line based on the CAFE31 software.

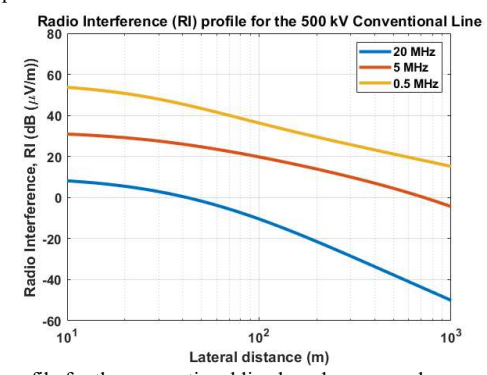


Fig. 6. RI profile for the conventional line based on our code.

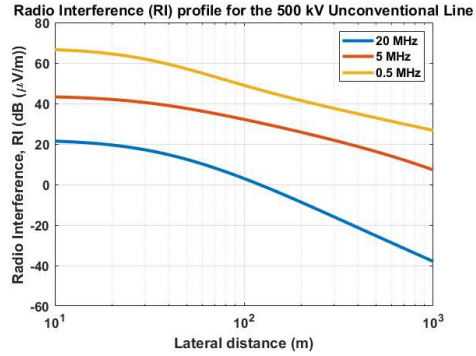


Fig. 7. RI profile for the unconventional line based on our code.

V. CONCLUSION

This paper discusses the effects of RI on transmission lines due to corona discharges occurring on high-voltage overhead transmission lines. We have also drawn a comparison between our recently proposed unconventional HSIL line and the conventional 500 kV transmission line and the effect of corona discharge on their RI profiles. We have shown a method of evaluating the RI profile for unconventional lines, which can help minimize its effects in the design stage.

REFERENCES

- [1] R. D. Begamudre, Extra High Voltage AC Transmission Engineering, Tunbridge Wells, Kent, UK: New Academic Science Limited, 2013.
- [2] M. Ghassemi, "High surge impedance loading (HSIL) lines: A review identifying opportunities, challenges, and future research needs," *IEEE Trans. Power Del.*, vol. 34, no. 5, pp. 1909–1924, 2019.
- [3] J. Hernandez *et al.*, "Electromagnetic transient performance of optimally designed high surge impedance loading lines," *IEEE Power & Energy Soc. General Meeting (PESGM)*, 2020, pp. 1-5.
- [4] M. Borghei and M. Ghassemi, "Geometrically optimized phase configurations and sub-conductors in the bundle for power transmission efficiency," *IEEE Electr. Insul. Conf. (EIC)*, 2019, pp. 295-299.
- [5] E. Larson et al., "Net-zero America: Potential pathways, infrastructure, and impacts," Interim Rep., Princeton University, Dec. 2020.
- [6] M. Abedin Khan and M. Ghassemi, "A new method for calculating electric field intensity on subconductors in unconventional high voltage, high power density transmission lines," *IEEE Conf. Electr. Insul. & Dielectr. Phenomena (CEIDP)*, 2023, pp. 1-4.
- [7] M. Abedin Khan and M. Ghassemi, "Compact unconventional overhead 500 kV transmission line for higher line loadability," *IEEE Power & Energy Society General Meeting (PESGM)*, 2025, pp. 1-5.
- [8] R. G. Olsen, High Voltage Overhead Transmission Line Electromagnetics-Volume II, Second Ed., 2018.
- [9] M. Abedin Khan and M. Ghassemi, "A new unusual bundle and phase arrangement for transmission line to achieve higher natural power," *IEEE North American Power Symp. (NAPS)*, 2023, pp. 1-5.
- [10] H. Wei-Gang, "Study on conductor configuration of 500-kV Chang-Fang compact line", *IEEE Trans. Power Del.*, vol. 18, no. 3, pp. 1002-8, 2003.
- [11] M. Abedin Khan and M. Ghassemi, "Calculation of audible noise and radio interference for unconventional high surge impedance loading (HSIL) transmission lines," *IEEE Conf. Electrical Insul. Dielectric Phenomena (CEIDP)*, 2023, pp. 1-4.
- [12] M. A. Khan and M. Ghassemi, "Corona loss calculation for unconventional high surge impedance loading transmission lines," *North American Power Symposium (NAPS)*, 2023, pp. 1-6.
- [13] B. Dhamala and M. Ghassemi, "Transmission expansion planning with high surge impedance loading lines at reduced voltage levels," *J. Modern Power Systems and Clean Energy*, doi: 10.35833/MPCE.2024.001149.
- [14] B. Dhamala and M. Ghassemi, "Smart transmission expansion planning based on the system requirements: A comparative study with unconventional lines," *Energies*, vol. 17, no. 8, p. 1912, 2024.
- [15] B. Dhamala and M. Ghassemi, "Comparative study of transmission expansion planning with conventional and unconventional high surge impedance loading (HSIL) lines," *IEEE Power & Energy Society General Meeting (PESGM)*, 2024, pp. 1-5.
- [16] B. Dhamala and M. Ghassemi, "Transmission expansion planning via unconventional high surge impedance loading (HSIL) lines," *IEEE North American Power Symposium (NAPS)*, 2023, pp. 1-6.
- [17] B. Dhamala and M. Ghassemi, "Unconventional high surge impedance loading (HSIL) lines and transmission expansion planning," *IEEE North American Power Symposium (NAPS)*, 2023, pp. 1-6.
- [18] B. Porkar, M. Ghassemi, and M. A. Khan, "Transmission expansion planning (TEP)-based unconventional high surge impedance loading (HSIL) line design concept," *IEEE North American Power Symposium* (NAPS), 2023, pp. 1-5.
- [19] M. A. Khan and M. Ghassemi, "Calculation of television interference (TVI) for unconventional high surge impedance loading (HSIL) transmission lines," *IEEE Conf. Electrical Insul. Dielectric Phenomena* (CEIDP), 2024, pp. 1-4
- [20] M. Abedin Khan, E. Arafat, S. Chowdhury, and M. Ghassemi, "Optimally located subconductors and phases to achieve transmission lines with high natural power and narrow corridor width," *IEEE Access*, vol. 13, pp. 7338-7352, 2025.
- [21] M. Ghassemi, M. Farzaneh, and W. A. Chisholm, "A coupled computational fluid dynamics and heat transfer model for accurate estimation of temperature increase of an ice-covered FRP live-line tool," *IEEE Trans. Dielectr. Electr. Insul.*, vol. 21, no. 6, pp. 2628-2633, 2014.
- [22] M. Ghassemi and M. Farzaneh, "Calculation of minimum approach distances for tools for live-line working under freezing conditions," *IEEE Trans. Dielectr. Electr. Insul.*, vol. 23, no. 2, pp. 987-994, 2016.